Biosensors and Bioelectronics 69 (2015) 100–105

Contents lists available at ScienceDirect

Biosensors and Bioelectronics

journal homepage: www.elsevier.com/locate/bios

A label-free electrochemical DNA biosensor based on covalent immobilization of salmonella DNA sequences on the nanoporous glassy carbon electrode

Mahmoud Amouzadeh Tabrizi, Mojtaba Shamsipur *

Department of Chemistry, Razi University, Kermanshah, Iran

ARTICLE INFO

Article history:
Received 15 January 2015
Received in revised form
12 February 2015
Accepted 13 February 2015
Available online 16 February 2015

Keywords:
Nanoporous glassy carbon electrode
Salmonella
Covalent immobilization
DNA biosensor
Label-free detection

ABSTRACT

Herein, an easy and cost-effective approach to the immobilization of probe was performed. The amino modified salmonella ssDNA probe sequence was covalently linked with carboxylic group on the surface of nanoporous glassy carbon electrode to prepare the DNA biosensor. The differential pulse voltammetry (DPV) and electrochemical impedance spectroscopy (EIS) techniques were used for the determination of salmonella DNA in the concentration ranges of 10–400 pM and 1–400 pM with limits of detection of 2.1 pM and 0.15 pM, respectively.

1. Introduction

Food borne diseases are a major public health and economic problem in the world. The Centers for Disease Control and Prevention (CDC) reported that only in the United States of America over 48 million people are sickened as a result of consuming contaminated foods or beverages (Scharff, 2011). According the European Centre for Disease prevention and Control (ECDC), salmonellosis is the second most common cause of food poisoning after campylobacter. The Economic Research Service (ERS) estimates that the annual economic cost of salmonellosis is 4.430 billion dollars (Scharff, 2011). Salmonella bacteria has been found in un-pasteurized milk, eggs, raw egg products, meat and poultry (Hoelzer et al., 2011). Therefore, it is necessary to develop a sensitive, selective and cost-effective method for determination of salmonella bacteria.

Recently, DNA detection methods have attracted considerable interest due to their early diagnosis of diseases. Up to now, numerous DNA detection methods have been reported in literature for the determination of salmonella, such as polymerase chain reaction (PCR) (Ma et al., 2014; Margot et al., 2013), rolling circle amplification (RCA) (Sato et al., 2013, 2010) and nucleic-acid sequence-based amplification (NASBA) (Mollasalehi and Yazdanparast, 2012, 2013). However, these methods are generally time-consuming, complex and expensive operations. To overcome these shortcomings, the electrochemical DNA biosensors are especially promising because of their simplicity, high sensitivity and selectivity (Erdem et al., 2006; Ligaj et al., 2014; Singh et al., 2013). It is well known that the electrochemical behaviors of DNA biosensors are related to the physico-chemical properties of the electrode surfaces. Several materials for the fabrication of electrochemical DNA biosensor have been reported in the literature (Hu et al., 2011; Peng et al., 2009; Rai et al., 2012; Yang et al., 2007; Zhang et al., 2013). Among them, the carbon based nanomaterials not only provide a large microscopic surface area for immobilization of bio-molecules, but also introduce a desirable biocompatible microenvironment (Gupta et al., 2013; Hu et al., 2011; Huang et al., 2014; Kim et al., 2012; Wang et al., 2011; Wei et al., 2010; Yola et al., 2014; Zhou et al., 2009). The nanoporous glassy carbon is one of these carbon based nanocomposites. The application of nanoporous glassy carbon electrode for the fabrication of electrochemical sensor (Geremedhin et al., 2013; Xu et al., 2010; Zhao et al., 2009) and biosensor (Haghighi and Tabrizi, 2011; Zhang et al., 1996) has been reported previously. To the best of our knowledge, the use of a nanoporous glassy carbon electrode for immobilization of DNA and its application as a DNA biosensor has not been yet reported. The DNA biosensor proposed in this work exhibited excellent electrochemical characteristics and high analytical performance in terms of sensitivity, stability, selectivity, linear range and limit of detection.

* Corresponding author. Fax: +98 831-4274580.
E-mail address: mshamsipur@yahoo.com (M. Shamsipur).

http://dx.doi.org/10.1016/j.bios.2015.02.024
0956-5663/

2. Experimental

2.1. Reagents and chemicals

All chemicals were of analytical reagent grade and used without further purification. Potassium dihydrogen phosphate (KH_2PO_4), potassium hydroxide (KOH), potassium chloride (KCl), hydrochloric acid (HCl), potassium hexacyanoferrate(III) ($K_3[Fe(CN)_6]$) and potassium hexacyanoferrate(II) ($K_4[Fe(CN)_6]$) were obtained from Merck (Darmstadt, Germany). N-(3-Dimethylaminopropyl)-*N*′-ethylcarbodiimide hydrochloride $C_8H_{17}N_3$.HCl (EDC.HCl) and N-hydroxysuccinimide (NHS, 98%) were obtained from Sigma–Aldrich (St. Louis, MO, USA). Double distilled water was used in all experiments. DNA oligonucleotides with the following sequences were obtained from Fazabiotech Co. (Tehran, Iran):

Probe single strand DNA (ssDNA):NH_2-5′-GGA GCT GCT GGC ATT ATT GAA-3′
Target DNA: 5′-TTC AAT AAT GCC AGC AGC TCC-3′

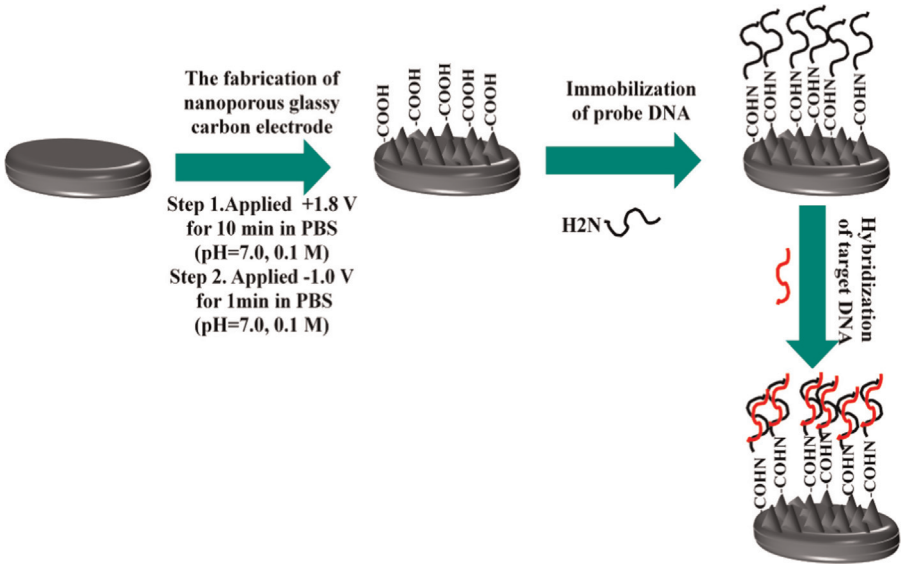

Scheme 1. The schematic illustration for fabrication of DNA biosensor.

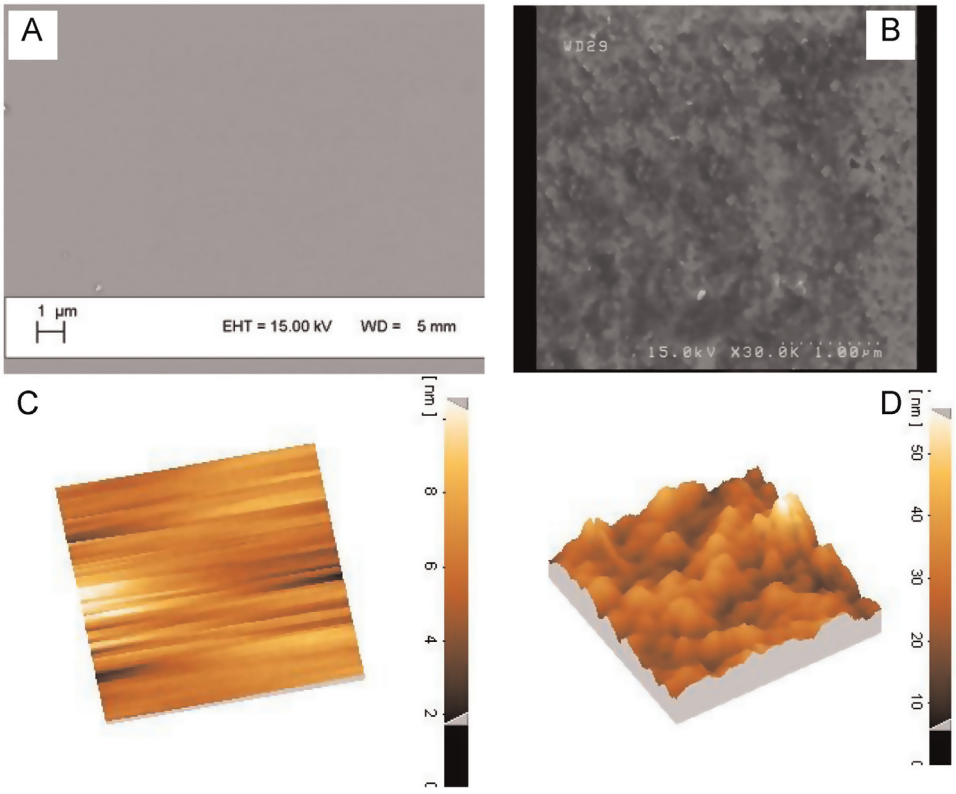

Fig. 1. SEM and AFM images of polished GCE (A,C) and the prepared GCE-red (B,D).

Double-base mismatched DNA: 5′-TTC AAT AAT GCT AGA AGC TCC-3′
Three-base mismatched DNA: 5′-TTC AAG AAT GCT AGC AGA TCC-3′
Non-complementary DNA: 5′-CAT CTC ATG GCC GAT TCG TTG-3′.
The photo tagging of components are added to the Supplementary section (Fig. S1).

2.2. Apparatus and measurements

Cyclic voltammetry (CV), electrochemical impedance spectroscopy (EIS) and differential pulse voltammetry (DPV) studies were performed using an μAutolab electrochemical system equipped with GPES and FRA 4.9 software (Eco-Chemie, Utrecht, The Netherlands). During the electrochemical measurements, the working electrode was a GCE-red/ssDNA set in cell device, and the auxiliary and reference electrodes were a Pt wire and Ag/AgCl electrode, respectively. Scanning electron microscopy (SEM) images were obtained using a Philips instrument, Model XL-30 at an accelerating voltage of 15.0 kV. Atomic force microscopy (AFM) images were obtained using a DME DualScope Scanner DS 95-200 (Herlev, Denmark).

2.3. Preparation of GCE-red/ssDNA and hybridization

The nanoporous glassy carbon was prepared according to the previously reported method without any modification (Zhao et al., 2008). In brief, the end surface of a GCE electrode (i.d.=3.0 mm, Azar Electrode, Urmia, Iran) was polished on a synthetic cloth successively with 0.3, 0.1 and 0.05 μm alumina slurry to obtain a mirror finish and then cleaned in water-ethanol solution (1:1) under ultrasonication. Next, the freshly polished GCE was anodized at 1.8 V in a 0.1 M KH_2PO_4 solution for 10 min to obtain the oxidized GCE (GCE-ox). The oxidized GCE was then reduced at −1.0 V in 0.1 M KH_2PO_4 for 1 min to obtain the reduced GCE (GCE-red). In this process, most of the oxygen-containing groups on the surface of oxidized GCE are reduced, while the carboxylic acid groups still remaining un-attacked (Engstrom and Strasser, 1984; Zhao et al., 2008). After that, the electrode was rinsed with 0.05 M phosphate buffer solution (PBS) thoroughly. Then the electrode was immersed in 0.05 M PBS of pH 7.0 containing 10 mM EDC and 20 mM NHS for 1 h to activate the carboxylic groups at the GCE-red. The electrode was then washed quickly with PBS and immediately immersed in a probe DNA solution (10 μM, 0.05 PBS of pH 7.0) for 2 h. Finally, the electrode (denoted as GCE-red/ssDNA) was thoroughly rinsed with deionized ultrafiltered water, dried in air and stored at 4 °C in 0.1 M PBS of pH 7.0 when not in use. In the next step, the GCE-red/ssDNA was transferred into the hybridization solution containing different concentrations of target DNA and incubated for 45 min at room temperature. After that, the electrode, denoted as GCE-red/dsDNA, was rinsed three times with water to remove the non-hybridized target. The schematic representation for the fabrication of proposed DNA biosensor is shown in Scheme 1.

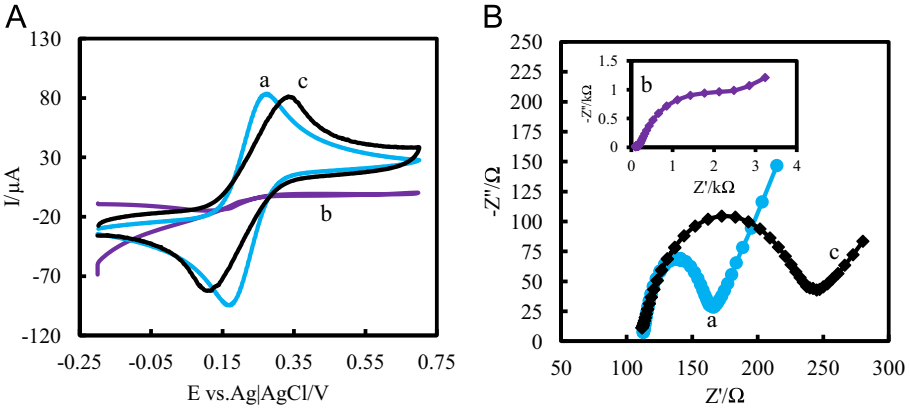

Fig. 2 Cyclic voltammograms (A) and Nyquist diagrams (B) of 5.0 mM $[Fe(CN)_6]^{3-/4-}$ in 0.1 M KCl recorded at (a) GCE, (b) GCE-ox and (c) GCE-red.

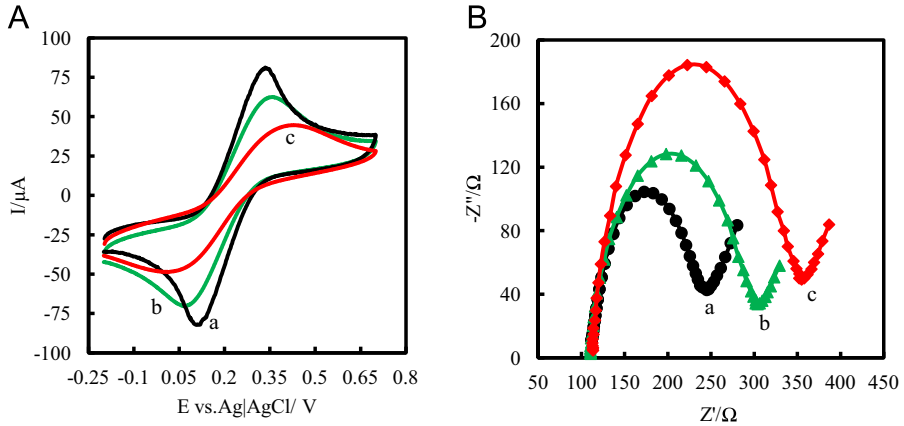

Fig. 3. Cyclic voltammograms (A) and Nyquist diagrams (B) of 5.0 mM $[Fe(CN)_6]^{3-/4-}$ in 0.1 M KCl recorded at (a) GCE-red, (b) GCE-red/ssDNA and (c) GCE-red/dsDNA.

3. Results and discussion

3.1. The surface characterization of GCE and GCE-red

The surface morphologies of the polished GCE and the prepared GCE-red were investigated using SEM and AFM (Fig.1). It is seen that the surface of reduced GCE (GCE-red) (B,D) was quite porous in comparison with the smooth surface of the GCE (A,C). Fig. S2 shows the surface profiles of both GCE and GCE-red. The maximum height of the roughness profile and root-mean-square deviation of the roughness profile for the GCE-red were 67.1 nm and 8.01 nm, respectively. While, the corresponding respective values for the polished GCE were 2.21 nm and 718 pm.

3.2. Electrochemical properties of the electrodes

The CV and EIS were used to characterize the interface properties of the electrodes surfaces, and the results are shown in Fig. 2. Fig. 2A shows the cyclic voltammograms (CVs) of GCE (a), GCE-ox (b) and GCE-red (c) in 0.1 M KCl solution containing 5.0 mM $K_3Fe(CN)_6^{-3/-4}$. It is seen that a pair of reversible redox peaks of $K_3Fe(CN)_6^{3-/4-}$ appeared at a bare GCE (a), but it disappeared at a oxidized GCE (b) because of strong electrostatic repulsing between oxygen groups on the surface of GCE-ox and the anionic probe. After electrochemical reduction, the pair of reversible redox peaks of $K_3Fe(CN)_6^{3-/4-}$ restored at the GCE-red (c). However, because of electrostatic repulsion between the remaining carboxyl functional groups on the surface of GCE-red and anionic redox probe, the peak separation of $K_3Fe(CN)_6^{3-/4-}$ on the GCE-red was larger than the freshly polished GCE.

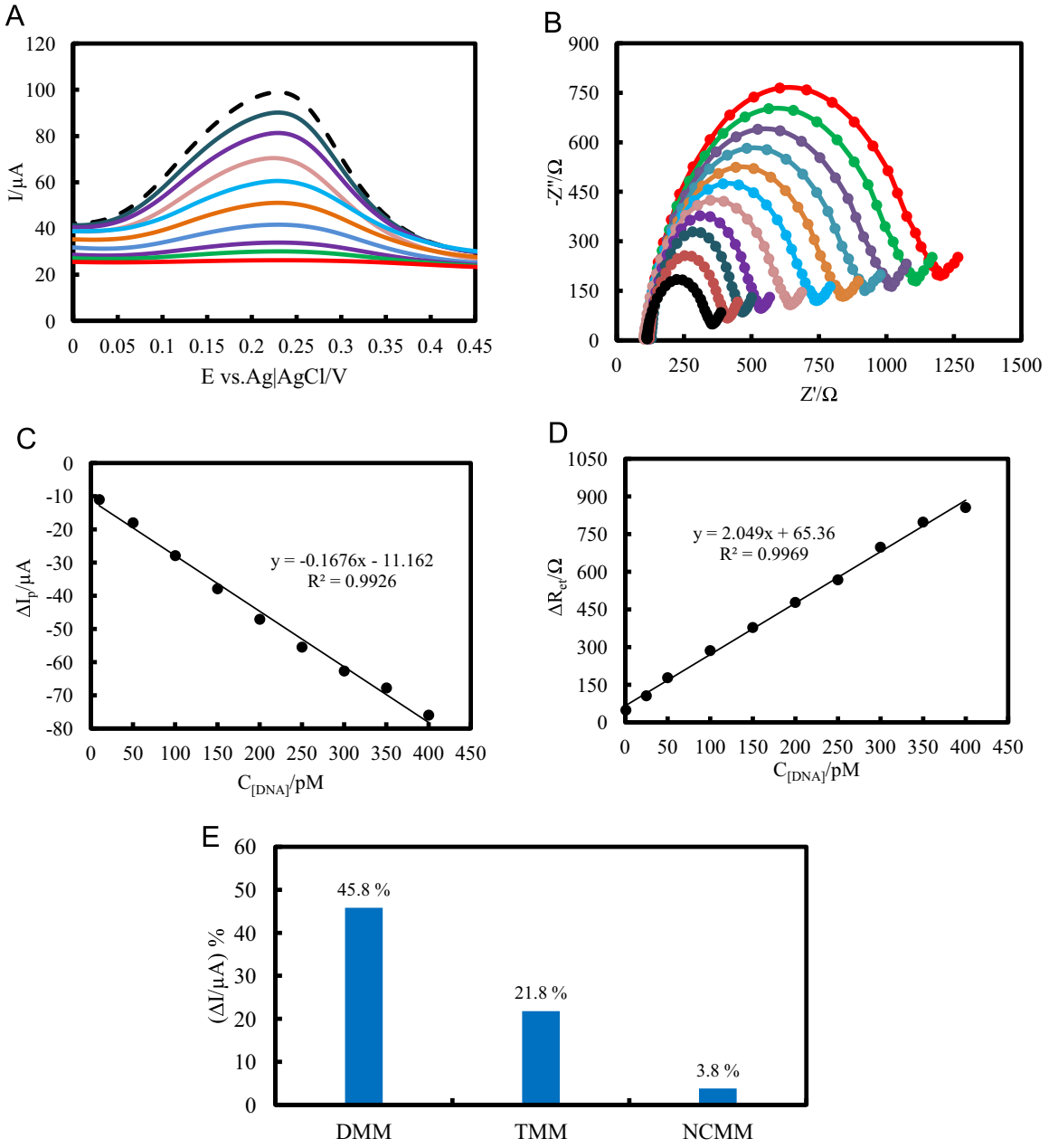

Fig. 4. DPV (A) and EIS (B) results for GCE-red/ss-DNA incubated with different concentrations of target DNA and calibration curves for ΔI_p (C) and ΔR_{et} (D) versus concentration of target DNA. (E) Comparison of hybridization signal intensities for GCE-red/ssDNA with 200 pM double-base mismatched (DMM), three-base mismatched (TMM) and non-complementary sequences (NCMM), respectively.

Table 1
Comparison of the analytical performance of the different salmonella DNA biosensors.

Probe	Method	Liner range/M	Limit of detection/M	RSD	References
GDH-DNA/CPE	AMP	5×10^{-8}–1×10^{-5}	5.0×10^{-8}	–	Ikebukuro et al. (2001)
ssDNA/Pt_{micro}electrode	EIS	1×10^{-9}–500×10^{-9}	1.0×10^{-9}	–	Berdat et al. (2008)
ssDNA/MCH/gold electrode	DPV	1×10^{-12}–10×10^{-9}	0.5×10^{-12}	5%	Li et al. (2012)
ssDNA/ Ru-Fe complex /GC electrode	SWV	0.4×10^{-6}–0.8×10^{-6}	0.4×10^{-6}	–	Díaz-Serrano et al. (2013)
ssDNA/SPCE	LSV	0.1×10^{-3}–15×10^{-3}	0.1×10^{-3}	–	Horakova-Brazdilova et al. (2008)
MB-labeled DNA probe/gold electrode	DPV	60×10^{-9}–300×10^{-9}	60.0×10^{-9}	–	Lai et al. (2006)
ssDNA/SA chip	SPR	5×10^{-9}–1000×10^{-9}	0.5×10^{-9}	–	Zhang et al. (2012)
ssDNA/gold electrode	ACV	25×10^{-9}–2400×10^{-9}	10×10^{-15}	–	Ferguson et al. (2009)
DNAzyme probe self-assembled gold nanoparticles	UV–vis	0.5×10^{-9}–50×10^{-9}	0.44×10^{-9}	5%	Luo et al. (2014)
ssDNA/GCE-red	DPV	10×10^{-12}–400×10^{-12}	2.1×10^{-12}	2.1%	This work
	EIS	1×10^{-12}–400×10^{-12}	0.15×10^{-12}		

GDH: glucose dehydrogenase CPE: Carbon paste electrode, AMP: Amperometry, EIS: Electro-chemical impedance spectroscopy, DPV: Differential pulse voltammetry, MCH: 6-mercapto-1-hexanol, Ru-Fe complex: $[Ru(Fe\text{-}Phen)_2dppz](PF_6)_2$, MB: Methylene blue, SPCE: Screen-printed carbon electrodes, SPR: Surface plasmon resonance, ACV: Alternating current voltammetry.

Fig. 2B displays the Nyquist plots obtained for a GCE (a), GCE-ox (b) and GCE-red (c) in a solution containing 5.0 mM $Fe(CN)_6^{3-/4-}$ couple (1:1) and 0.1 M KCl. Obviously, the impedance of GCE-ox is dramatically increased from 63 Ω to 5327 Ω, which indicates that the conductivity of GCE has been declined by the electrochemical oxidation of GCE surface. However, after the electrochemical reduction of oxidized GCE, the value of R_{et} decreased to154 Ω. These results were consistent with the CV results. All these results demonstrated that the surface property of glassy carbon electrode changed considerably after the electrochemical treatment.

The CV and EIS were also used to characterize the assembled process of the biosensor in 5.0 mM $Fe(CN)_6^{3-/4-}$, and the results are shown in Fig. 3A and B, respectively. Fig. 3A displays the CV behavior of $Fe(CN)_6^{3-/4-}$ on the GCE-red (a), GCE-red/ssDNA (b) and GCE-red/dsDNA (c). It can be clearly observed that the peak current was largely decreased when the probe ssDNA was assembled on the surface of the GCE-red (b) and after the probe DNA was hybridized with the target DNA, the peak current continuously decreased (c). The reasonable explanation is that after the probe DNA was hybridized with target DNA, the density of negative charges at the electrode surface increased, leading to a further decrease in peak current and increase in peak to peak separation because of the strong electrostatic repulsion interaction between DNA and $Fe(CN)_6^{3-/4-}$.

Fig. 3B displays the EIS behavior of $Fe(CN)_6^{3-/4-}$ on the GCE-red (a), GCE-red/ssDNA (b) and GCE-red/dsDNA (c). As seen, after immobilization of the capture DNA, the value of R_{et} increased from 154 to 219.0 Ω. Subsequently, the target DNA was hybridized with target DNA resulted in increased R_{et} to 269 Ω. These results were consistent with the CVs results.

3.3. Voltammetric and impedimetric detection of target DNA

The analytical calibration was performed using various concentrations of target DNA to evaluate the sensitivity of the fabricated biosensor. As can be seen from Fig. 4A and C the DPV responses linearly decreased with the increasing target DNA concentration over the range of 10-400 pM with a regression equation of i_p (μA) = −0.16 $C_{[DNA]}$ (pM) −11.16 and a correlation coefficient of 0.9926. The limit of detection (LOD) of this method was 2.1 pM ($3\sigma/S$). A corresponding table including the concentrations that have been used and the values of concentrations that were actually measured/estimated with this biosensor are added to the supplementary section (Table S1).

Due to the high ability of EIS technique for probing the interfacial properties at the electrode surface and the possibility of performing label-free detections, EIS measurement was also applied as an efficient alternative detection system to further confirm the analytical performance of the biosensor. As shown in Fig. 4B and D, the increase in R_{et} were found to be linearly proportional to the target DNA concentrations in the tested range of 1–400 pM give a linear profile with a regression equation of ΔR_{et} (Ω) = 2.049 $C_{[DNA]}$ (pM) + 65.36 (R_2 = 0.9969) and a limit of detection of 0.15 pM ($3\sigma/S$), which was largely improved over that of the DPV measurements. The results indicated that the label-free electrochemical strategy based on nanoporous glassy carbon electrode exhibited high sensitivity, which may be attributed to its high surface area.

The selectivity of the proposed DNA biosensor for target detection was studied by using double-base mismatched (DMM) and three-base mismatched (TMM) and a non-complementary matched (NCMM) strands, using the DPV method and the results for are shown in Fig. 4E. As seen, the corresponding ΔI values at an equimolar concentration of 200 pM with DNA were 45.8% (DMM), 21.4% (TMM) and 3.80% (NCMM).

Additionally, in Table 1 are compared the linear rang and limit of detection of the proposed salmonella DNA biosensor with those of different methods previously reported in the literature. As is obvious from Table 1, in most cases, the proposed GCE-red/ssDNA biosensor shows an improved analytical behavior over that of the previously reported systems.

The stability of the probe DNA at the platform surface plays an important role in obtaining high performance biosensors. The stability of the GCE-red/ssDNA biosensor was then evaluated by measuring its DPV response at the electrode in 0.1 M PBS of 7.0. The relative standard deviation (RSD) was found to be 2.1% after five successive scans. When not in use, the GCE-red/ssDNA biosensor was stored at 4 °C in 0.1 M PBS of pH 7.0, no measurable change for the DPV response was observed after 10 days. This high stability is mainly attributed to the covalent immobilization of DNA at the surface of GCE-red, which possesses an excellent biocompatibility.

4. Conclusions

In summary, a novel, simple and ultrasensitive label-free electrochemical DNA biosensor for salmonella bacteria base on immobilization of the amino terminal of the DNA probe sequence, via EDC and NHS, on the surface of a nanoporous glassy carbon electrode was constructed and used successfully for sensing of DNA hybridization. The resulting carboxylic acid groups and nanoporous structure of GCE-red provided a suitable platform for covalent immobilization of the DNA sequence. The experimental results obtained by DPV and EIS techniques indicated that the proposed biosensor display reasonable stability, good

reproducibility and selectivity and high sensitivity for picomolar detection of the target DNA.

Acknowledgements

The authors thank the Research Council of Razi University (Kermanshah, Iran) and Iran National Elites Foundation (INEF) for the support of this work.

Appendix A. Suplementary Information

Supplementary data associated with this article can be found in the online version at http://dx.doi.org/10.1016/j.bios.2015.02.024.

References

Berdat, D., Martin Rodriguez, A.C., Herrera, F., Gijs, M.A.M., 2008. Lab Chip 8, 302–308.
Díaz-Serrano, M., Rosado, A., Santana, D., Vega, E.Z., Guadalupe, A.R., 2013. J. Phys. Conf. Ser. 421, 012008.
Engstrom, R.C., Strasser, V.A., 1984. Anal. Chem. 56, 136–141.
Erdem, A., Pividori, M.I., Lermo, A., Bonanni, A., Valle, Md, Alegret, S., 2006. Sens. Actuators B Chem. 114, 591–598.
Ferguson, B.S., Buchsbaum, S.F., Swensen, J.S., Hsieh, K., Lou, X., Soh, H.T., 2009. Anal. Chem. 81, 6503–6508.
Geremedhin, W., Amare, M., Admassie, S., 2013. Electrochim. Acta 87, 749–755.
Gupta, V.K., Yola, M.L., Qureshi, M.S., Solak, A.O., Atar, N., Üstündağ, Z., 2013. Sens. Actuators B Chem. 188, 1201–1211.
Haghighi, B., Tabrizi, M.A., 2011. Electrochim. Acta 56, 10101–10106.
Hoelzer, K., Moreno Switt, A., Wiedmann, M., 2011. Vet. Res. 42, 1–27.
Horakova-Brazdilova, P., Fojtova, M., Vytras, K., Fojta, M., 2008. Sensors 8, 193–210.
Hu, Y., Hua, S., Li, F., Jiang, Y., Bai, X., Li, D., Niu, L., 2011. Biosens. Bioelectron. 26, 4355–4361.
Huang, K.-J., Liu, Y.-J., Wang, H.-B., Wang, Y.-Y., 2014. Electrochim. Acta 118, 130–137.
Ikebukuro, K., Kohiki, Y., Sode, K., 2001. Biosens. Bioelectron. 17, 1075–1080.
Kim, B., Lee, J., Namgung, S., Kim, J., Park, J.Y., Lee, M.-S., Hong, S., 2012. Sens. Actuators B Chem. 169, 182–187.
Lai, R.Y., Lagally, E.T., Lee, S.-H., Soh, H.T., Plaxco, K.W., Heeger, A.J., 2006. PNAS 103, 4017–4021.
Li, Q., Cheng, W., Zhang, D., Yu, T., Yin, Y., Ju, H., Ding, S., 2012. Int. J. Electrochem. Sci. 7, 844–856.
Ligaj, M., Tichoniuk, M., Gwiazdowska, D., Filipiak, M., 2014. Electrochim. Acta 128, 67–74.
Luo, R., Li, Y., Lin, X., Dong, F., Zhang, W., Yan, L., Cheng, W., Ju, H., Ding, S., 2014. Sens. Actuators B Chem. 198 (0), 87–93.
Ma, K., Deng, Y., Bai, Y., Xu, D., Chen, E., Wu, H., Li, B., Gao, L., 2014. Food Control 42, 87–93.
Margot, H., Stephan, R., Guarino, S., Jagadeesan, B., Chilton, D., O'Mahony, E., Iversen, C., 2013. Int. J. Food Microbiol. 165, 221–226.
Mollasalehi, H., Yazdanparast, R., 2012. Anal. Biochem. 425, 91–95.
Mollasalehi, H., Yazdanparast, R., 2013. Anal. Chim. Acta 770, 169–174.
Peng, H., Zhang, L., Soeller, C., Travas-Sejdic, J., 2009. Biomaterials 30, 2132–2148.
Rai, V., Deng, J., Toh, C.-S., 2012. Talanta 98, 112–117.
Sato, K., Ishii, R., Sasaki, N., Sato, K., Nilsson, M., 2013. Anal. Biochem. 437 (1), 43–45.
Sato, K., Tachihara, A., Renberg, B., Mawatari, K., Sato, K., Tanaka, Y., Jarvius, J., Nilsson, M., Kitamori, T., 2010. Lab Chip 10, 1262–1266.
Scharff, R., 2011. J. Food Prot. 75, 123–131.
Singh, A., Sinsinbar, G., Choudhary, M., Kumar, V., Pasricha, R., Verma, H.N., Singh, S. P., Arora, K., 2013. Sens. Actuators B Chem. 185, 675–684.
Wang, Z., Zhang, J., Chen, P., Zhou, X., Yang, Y., Wu, S., Niu, L., Han, Y., Wang, L., Chen, P., Boey, F., Zhang, Q., Liedberg, B., Zhang, H., 2011. Biosens. Bioelectron. 26, 3881–3886.
Wei, Q., Mao, K., Wu, D., Dai, Y., Yang, J., Du, B., Yang, M., Li, H., 2010. Sens. Actuators B Chem. 149, 314–318.
Xu, X., Feng, Y., Li, J., Li, F., Yu, H., 2010. Biosens. Bioelectron. 25, 2324–2328.
Yang, J., Yang, T., Feng, Y., Jiao, K., 2007. Anal. Biochem. 365, 24–30.
Yola, M.L., Eren, T., Atar, N., 2014. Electrochim. Acta 125, 38–47.
Zhang, D., Yan, Y., Li, Q., Yu, T., Cheng, W., Wang, L., Ju, H., Ding, S., 2012. J. Biotechnol. 160 (3–4), 123–128.
Zhang, W., Zong, P., Zheng, X., Wang, L., 2013. Biosens. Bioelectron. 42, 481–485.
Zhang, Z., Lei, C., Sun, W., Liu, H., Deng, J., 1996. J. Electroanal. Chem. 419, 85–91.
Zhao, Q.-L., Bao, L., Luo, Q.-Y., Zhang, M., Lin, Y., Pang, D.-W., Zhang, Z.-L., 2009. Biosens. Bioelectron. 24 (10), 3003–3007.
Zhao, Q.-L., Zhang, Z.-L., Bao, L., Pang, D.-W., 2008. Electrochem. Commun. 10, 181–185.
Zhou, N., Yang, T., Jiang, C., Du, M., Jiao, K., 2009. Talanta 77, 1021–1026.